MOLECULAR AND CELLULAR BIOLOGY, Apr. 2011, p. 1432–1443 Vol. 31, No. 7
0270-7306/11/$12.00 doi:10.1128/MCB.00451-10
Copyright © 2011, American Society for Microbiology. All Rights Reserved.

A Novel *Gli3* Enhancer Controls the *Gli3* Spatiotemporal Expression Pattern through a TALE Homeodomain Protein Binding Site▽‡

Sarah Coy,[1]† Jorge H. Caamaño,[2] Jaime Carvajal,[3] Michael L. Cleary,[4] and Anne-Gaëlle Borycki[1]*

Department of Biomedical Science, University of Sheffield, Sheffield S10 2TN, United Kindgom[1]; IBR-MRC Centre for Immune Regulation, University of Birmingham Medical School, Birmingham B15 2TT, United Kingdom[2]; Section of Gene Function and Regulation, The Institute of Cancer Research, London SW3 6JB, United Kingdom[3]; and Department of Pathology, Stanford University School of Medicine, Stanford, California 94305[4]

Received 16 April 2010/Returned for modification 25 May 2010/Accepted 17 January 2011

The zinc finger transcription factor Gli3 is an essential mediator of hedgehog signaling. *Gli3* has a dynamic expression pattern during embryonic development. In the neural tube, *Gli3* transcripts are patterned along the anteroposterior and dorsoventral axes such that the initial broad expression in the posterior neural tube becomes dorsally restricted as neurogenesis takes place. Little is known about the molecular mechanisms that regulate this dynamic expression. Here, we report on a phylogenetic analysis of the *Gli3* locus that uncovered a novel regulatory element, HCNE1. HCNE1 contains a compound Pbx/Meis binding site that binds Pbx and Meis/Prep proteins *in vitro* and *in vivo*. We show that HCNE1 recapitulates *Gli3* expression in the developing neural tube and that mutations in the Pbx/Meis binding site affect the spatiotemporal control of HCNE1 transcriptional activity. Ectopic expression or loss of function of Pbx and Meis/Prep proteins in the chick and mouse embryo results in aberrant expression of endogenous *Gli3* transcripts. We propose a novel role for TALE proteins in establishing the correct spatiotemporal expression pattern of *Gli3* in the vertebrate spinal cord, thus implicating TALE transcription factors in early embryonic patterning events controlled by Sonic hedgehog signaling.

Sonic hedgehog (Shh) is an essential signaling molecule for embryonic and fetal development. In the absence of Shh signaling, embryonic tissues and organs, including the ventral neural tube, limb, somites, eye, kidneys, and lungs, fail to develop or are abnormally patterned (48). Sonic hedgehog signals are transduced in receiving cells through the Gli proteins, which are zinc finger-containing transcription factors. Three vertebrate Gli genes have been identified, encoding Gli1, Gli2, and Gli3 (36, 37, 59). *In vitro* and *in vivo* studies indicate that while Gli2 and Gli3 are primary mediators of immediate-early response to Shh signals, Gli1 acts as a secondary mediator (33). Consistent with this, Gli1 is a transcriptional target of Shh signaling (26, 40, 41). Moreover, while Gli2 and Gli3 have retained the evolutionarily conserved transcriptional duality present in their *Drosophila* counterpart, *Cubitus interruptus*, Gli1 acts only as a transcriptional activator whose activity is mostly dispensable during embryonic development (6, 7, 55, 61, 69, 71). Among Gli proteins, Gli3 has unique characteristics. First, genetic studies have established that Gli3 acts primarily as a repressor in many Shh-controlled organs, including the neural tube, limb, and somites, although an inducing activity is revealed in the absence of Gli2 (7, 42, 47, 56). Second, there is evidence that Gli3 functions also in a hedgehog-independent manner in tissue patterning during embryogenesis (65). One possibility is that Gli3 may interfere directly or indirectly with the activity of other signaling pathways, such as Wnt and BMP (43, 52, 67). Finally, Gli3 dosage is critical as mouse and human heterozygous individuals display phenotypic defects. Indeed, a number of human syndromes resulting in limb deformity and craniofacial abnormalities are associated with autosomal dominant mutations in the Gli3 locus, including Greig cephalopolysyndactyly syndrome (GCPS) (34, 70, 72), Pallister-Hall syndrome (PHS) (35), postaxial polydactyly type A (PAPA) (58), and preaxial polydactyly type IV (PPD-IV) (57).

Thus, correct spatiotemporal expression of *Gli3* is critical to ensure accurate hedgehog signaling levels and normal organogenesis. This is evidenced by the near-normal phenotype of the $Shh^{-/-}$; $Gli3^{-/-}$ spinal cord compared to the $Shh^{-/-}$ spinal cord, which indicates that the primary role of Shh in the neural tube is to antagonize Gli3 repressor activity and that excessive Gli3 repressor activity is deleterious for ventral neural cell-type formation (42). Consistent with this, ectopic *Gli3* expression inhibits the formation of ventral neural cell types (49, 56). Gli3 repressor activity is normally confined to the dorsal neural tube, because *Gli3* is dynamically expressed and subject to spatiotemporal control during neural tube formation. Initially expressed throughout the neural tube, *Gli3* becomes restricted to the dorsal neural tube as development proceeds (3, 14). This dorsal restriction appears to be controlled by Shh signaling, although there is no evidence for a direct regulation of Shh on *Gli3* expression (14). While significant progress has been made on the biochemistry and biological function of the Gli proteins, the molecular mechanisms controlling *Gli* gene expression during embryogenesis remain to be elucidated. *Gli1* transcription,

* Corresponding author. Mailing address: Department of Biomedical Science, Firth Court, Western Bank, Sheffield S10 2TN, United Kingdom. Phone: (44) 114 222 2701. Fax: (44) 114 276 5413. E-mail: a.g.borycki@sheffield.ac.uk.

† Present address: Department of Biochemistry, University of Oxford, South Parks Road, Oxford OX1 3QU, United Kingdom.

‡ Supplemental material for this article may be found at http://mcb.asm.org/.

▽ Published ahead of print on 24 January 2011.

with its restricted expression adjacent to Shh sources, requires Gli2 and Gli3 activity (26, 41, 47, 68). In contrast, *Gli2* and *Gli3* dynamic expression patterns in the vertebrate embryo (14, 40, 45, 47, 50) suggest that multiple regulatory elements and combinatorial mechanisms may be at play to control their transcription. Consistent with this hypothesis, previous studies have identified several intragenic sequences that are conserved among vertebrates (1–3, 54). Although several of the elements identified previously drive expression in the neural tube, none of them appear to fully reproduce *Gli3* dynamic expression pattern, in particular its dorsal restriction. Therefore, additional elements not reported so far must exist and participate in the control of the *Gli3* spatiotemporal expression pattern. Here, we used a similar phylogenetic footprinting approach and identified 11 novel highly conserved noncoding elements (HCNEs) in the *Gli3* locus (64). Using a reporter gene expression assay in the chick neural tube, we show that a novel uncharacterized HCNE, HCNE1, generates a reporter gene expression pattern similar to that of *Gli3*. HCNE1 contains two conserved binding sites for TALE homeodomain transcription factors, and our *in vitro* and *in vivo* studies show that TALE proteins of the Pbx and Prep family bind one of these sites and shape HCNE1-derived reporter gene expression as well as endogenous *Gli3* expression in the neural tube. Conversely, mutations in the TALE binding sites and misexpression of dominant-negative TALE constructs or analysis of *Pbx1* mutant mouse embryos indicate that TALE protein binding and activity are required to control the onset of *Gli3* expression and generate the *Gli3* dynamic expression pattern. These results suggest that the correct spatiotemporal pattern of *Gli3* and HCNE1-mediated reporter gene expression is directly controlled by members of the TALE homeodomain protein family. Together, these data provide novel insights into the regulation of *Gli3* and suggest a mechanism by which TALE proteins may integrate control of hedgehog response with control of cell fate specification.

MATERIALS AND METHODS

Cell culture. The rat pheochromocytoma PC12 cell line was grown in RPMI 1640 (Sigma) supplemented with 10% fetal bovine serum (FBS; Invitrogen), 5% fetal horse serum (FHS; Invitrogen), and 1% L-glutamine (Invitrogen). The human medulloblastoma DAOY cell line was grown in Dulbecco's modified Eagle's medium (DMEM; Gibco) supplemented with 10% FBS (Invitrogen) and 1% L-glutamine (Invitrogen). Cells were grown at 37°C in the presence of 5% CO_2.

Mice. *Pbx1*$^{+/-}$ mice were maintained as heterozygotes and genotyped as previously described (62). Heterozygous animals were crossed to produce *Pbx1*$^{-/-}$ embryos. Embryonic day 0.5 (E0.5) was the day that vaginal plugs were found.

5′ RACE. One microgram of total E9.5 mouse embryo RNA was used to prepare 5′ rapid-amplification-of-cDNA-ends (5′ RACE)-ready cDNA using a Smart RACE cDNA amplification kit (Clontech). RACE was carried out according to the manufacturer's protocol, using Gli3-specific primers in exon 3 and exon 2 (data available on request). Fragments amplified were cloned into the pCR-TOPOII vector (Invitrogen) and sequenced.

Genomic sequence analyses. Genomic sequences at the Gli3 locus for various vertebrate species were retrieved from the Ensembl database (www.ensembl.org/) (32). Pairwise alignments were generated using the AVID alignment tool (15, 24) and visualized on the VISTA genome server (www-gsd.lbl.gov/vista/) and the ECR genome browser (http://ecrbrowser.dcode.org/). Transcription factor binding sites were identified using the MatInspector tool from Genomatix (www.genomatix.de/).

Reporter constructs. Putative enhancers (HCNEs) were amplified by PCR from mouse genomic DNA using Expand high-fidelity *Taq* polymerase (Roche) and subcloned into the LacZ reporter construct nP1230, which expresses β-galactosidase (β-Gal) under the control of the human β-globin promoter. Sequences were chosen on the basis of their conserved homology in human, mouse, and chick genomes. nP1230 was a modified version of p1230 (74), in which a nuclear localization signal (3xnls) from pCIG was introduced upstream of β-galactosidase. In our hands, the human β-globin promoter gave lower basal transcriptional levels than similar constructs driven by the thymidine kinase promoter. Site-directed mutagenesis was carried out in accordance with the protocol described in the QuikChange site-directed mutagenesis kit (Stratagene), using Phusion Hot Start high-fidelity DNA polymerase (Finnzymes). Primers for site-directed mutagenesis were designed using the QuikChange primer design program (Stratagene). All constructs were verified by sequencing using a BigDye Terminator v3.1 cycle sequencing kit (Applied Biosystems) and run on an ABI 3730 capillary sequencer (Applied Biosystems) by the University of Sheffield Core Genomics service. The primers used are available on request.

Electromobility shift assay (EMSA). Nuclear extract was prepared from Hamburger-Hamilton (HH) stage 12 chicken embryos (150 embryos) or from cell lines (10 75-cm^2 flasks), pelleted, resuspended, and homogenized in 0.4 ml buffer A (10 mM HEPES [pH 7.9], 10 mM KCl, 0.1 mM EDTA, 0.1 mM EGTA, 1 mM dithiothreitol [DTT], 2 μg aprotinin, 2 μg leupeptin, 750 μM phenylmethylsulfonyl fluoride [PMSF]). After 15 min of incubation on ice, lysis was triggered by the addition of 10% NP-40, and following centrifugation at 4,000 rpm, cytoplasmic extracts present in the supernatant were collected and frozen in liquid nitrogen. Pellets were resuspended in 50 ml buffer C (20 mM HEPES [pH 7.9], 0.1 mM EDTA, 0.1 mM EGTA, 0.4 M NaCl, 1 mM DTT, 5 μg aprotinin, 2 μg leupeptin, 2 mM PMSF). After centrifugation at 4,000 rpm, nuclear extracts present in the supernatant were collected and stored in liquid nitrogen. Proteins (Pbx1b, Prep1, and Prep2) were prepared using a TnT quick coupled transcription/translation system (Promega) in accordance with the manufacturer's instructions. Oligonucleotides were radiolabeled by fill-in using [^{32}P]dCTP (3,000 Ci/mmol; NEN) and Klenow (Roche). Labeled oligonucleotides were purified on a Sephadex G25 column (Roche). Nuclear extracts (1.5 μg) or *in vitro*-translated proteins were incubated with 400,000 cpm of ^{32}P-labeled oligonucleotides and 2 μg of poly(dI-dC) in BC100 buffer (20 mM HEPES [pH 7.9], 100 mM KCl, 5 mM $MgCl_2$, 1 mM DTT, 17% glycerol) for 15 min at room temperature. Where indicated, cold oligonucleotides and/or antibodies were added to the binding reaction. The antibodies used were anti-Pbx1/2/3/4 (H-260; sc-25411X), anti-Pbx1b (41.1; sc101852), anti-Prep1 (B-2; sc25282X), and anti-Prep2 (P-20; sc55889X) (Santa Cruz Biotechnology). Complexes were analyzed by electrophoresis on a 5.5% polyacrylamide gel run in 0.25× Tris-borate-EDTA buffer. Following electrophoresis, gels were dried and exposed to Kodak Biomax XAR film at −80°C.

Chick neural tube electroporation. Fertilized white Leghorn chicken eggs (Winter egg farm) were incubated at 39°C and staged according to the Hamburger-Hamilton (HH) staging method (30). HH stage 10 and 11 chicken embryos were coelectroporated with a solution containing reporter constructs and the control plasmid pMES-EGFP (21) at a ratio of 3:1. The En-Meis1a and Meis1a-VP16 constructs (kindly donated by R. Maas) are N-terminal fusion proteins of the *Drosophila* En repressor domain and C-terminal fusion proteins of the activation domain of virion protein 16 (VP16) of herpes simplex virus with mouse Meis1a, respectively (75). Electrodes (5 mm L-shaped gold; Genetronics, Inc.) were placed on each side of the neural tube, and 5 pulses of 24 V and 30 ms each were delivered at 500-ms intervals using a BTX ECM 830 square wave generator. Green fluorescent protein (GFP) levels were examined at 12 to 24 h postelectroporation under a Leica MZ160F fluorescence stereomicroscope. Embryos with strong GFP expression throughout the anteroposterior axis were retained for analysis.

LacZ staining. Embryos were fixed in 1% paraformaldehyde (PFA) for 30 to 60 min at room temperature, washed in LacZ rinse solution (5 mM EGTA, 0.01% sodium deoxycholate, 0.02% NP-40 [Igepal], 2 mM $MgCl_2$ in phosphate-buffered saline [PBS]), and stained for 8 h in LacZ rinse solution containing 10 mM $K_3Fe(CN)_6$, 10 mM $K_4Fe(CN)_6$, and 1 mg/ml 5-bromo-4-chloro-3-indolyl-β-D-galactopyranoside (X-Gal; Invitrogen).

Reverse transcription-PCR (RT-PCR). Total RNA was isolated from HH stage 12 chicken embryos and DAOY and PC12 cells by use of TRIzol reagent (Gibco) in accordance with the manufacturer's protocol. cDNAs were prepared using a Superscript first-strand synthesis kit (Invitrogen). All products were amplified by PCR using BioMix Red (Bioline) in an Eppendorf PCR machine. The primers used are available on request. The identity of the PCR products was confirmed by cloning them into the TOPO-pCRII vector (Invitrogen) and sequencing them.

***In situ* hybridization.** Embryos were fixed in 4% paraformaldehyde. They were then either embedded in 2% agarose in PBS, in which case transverse sections were obtained using a Vibratome 1500 (Vibratome), or directly processed for

whole-mount *in situ* hybridization. *In situ* hybridization was essentially performed as previously described (47). A 900-bp cDNA fragment of quail *Gli3*, a 926-bp cDNA fragment of mouse *Gli3*, a 788-bp cDNA fragment of chick *Pbx1* (25), a 9,901-bp cDNA fragment of chick *Prep1* (25), and a 1,059-bp cDNA fragment of chick *Prep2* (25) were used as probes and labeled with digoxigenin (DIG) using a DIG RNA labeling kit (Roche) according to the manufacturer's manual. Mouse embryos of different genotypes were marked with small cuts and then processed together in the same tube to ensure equal treatment during the hybridization procedure. Stained embryos were photographed on an MZ12.5 stereomicroscope (Leica) using a Spot Insight camera (Diagnostic Instruments) with Spot Advanced digital image capture software. Following whole-mount *in situ* hybridization, transverse sections were generated using a Vibratome 1500 and mounted in Glycergel (Dako Cytomation). Images were captured on a DMR microscope (Leica) using a DC300FX digital camera (Leica) and the Leica IM50 image capture software program.

Immunohistochemistry. Embryos were embedded and processed for immunofluorescence as described previously (4). The antibodies used in this study were mouse anti-β-galactosidase (Promega) at 1:1,000 and Alexa Fluor 594-conjugated goat anti-mouse IgG (A11005; Molecular Probes) at 1:2,000. Images were captured on an SP1 laser-scanning confocal microscope (Leica) and processed using the ImageJ and Photoshop (Adobe) software programs.

ChIP. E10.5 mouse embryo chromatin was cross-linked for 30 min at room temperature in PBS containing 1.85% formaldehyde. Fixation was quenched by the addition of a 1/20 volume of glycine. Chromatin immunoprecipitation (ChIP) was performed as described previously (31), with the following modifications. Sonication buffer contained 1% sodium deoxycholate and 1% SDS, and lysates were cleared by incubating the samples overnight with 30 μl protein G beads previously washed in PBS containing 0.5% BSA. For the ChIP reaction, 9.25 μg chromatin and 3 μg antibody were incubated at 4°C for 2 h in 450 μl sonication buffer to allow binding. The antibodies were anti-Pbx1/2/3/4 (H-260; sc-25411X) and anti-Meis1/2 (H-80; sc-25412 X) (Santa Cruz Biotechnology). Immune complexes were collected by adsorption to protein G beads for 6 h at 4°C. Beads were washed twice with sonication buffer, twice with sonication buffer containing 500 mM NaCl, twice with 20 mM Tris (pH 8.0)–1 mM EDTA–250 mM LiCl–0.5% NP-40–0.5% sodium deoxycholate, and twice with Tris-EDTA buffer. Immunocomplexes were eluted with 200 μl elution buffer (50 mM [pH 8], 1 mM EDTA, 1% SDS, 50 mM $NaHCO_3$) by incubation in a rotating oven at 65°C for 10 min. Beads were pelleted by centrifugation at 13,000 rpm for 1 min, and supernatants containing chromatin were recovered. This elution process was repeated such that the final volume of recovered supernatant was 400 μl. Twenty microliters of 4 M NaCl was added to the supernatant, and samples were incubated at 65°C overnight. Finally, the DNA was successively treated with 10 μg RNase A for 1 h at 37°C with 20 μg proteinase K for 2 h at 42°C, extracted with phenol-chloroform, and precipitated. Pellets were resuspended in 50 μl H_2O. Immunoprecipitated DNA and input DNA were analyzed by PCR using HCNE1-specific primers (data available on request). Amplifications (35 cycles) were performed in the presence of 1 μl dimethyl sulfoxide (DMSO) to generate a 441-bp product.

Transactivation assay. HELA cells were maintained in Dulbecco's modified Eagle's medium (DMEM) supplemented with 10% fetal calf serum, penicillin-streptomycin (Sigma), and 4 mM glutamine (Sigma) in 5% CO_2 at 37°C. Before transient transfection, cells were transferred into Opti-MEM medium in 24-well plates and transfected using Lipofectamine 2000 (Invitrogen). For each transfection, 300 ng of a β-Gal reporter construct and 200 ng of a pGL3 reporter construct were used, alongside 250 ng mPbx1b and mPrep2 in the pCDNA3 vector. The final amount of DNA in the transfection mix was made up to 1 μg by the addition of empty pCDNA3 vector. All transfections were performed in triplicate. Transactivation assays were performed 24 h after transfection, using the dual-light combined reporter gene assay system (Applied Biosystems), using 50 μl lysis solution per well, and chemiluminescence detection was performed using a Sirius luminometer. The values shown are the fold inductions of the average β-galactosidase activity, normalized to the level for firefly luciferase activity from the pGL3 reporter plasmid, following transfection in the presence of Prep2 and Pbx1b expression vectors, compared with the average obtained in the absence of Prep2 and Pbx1b expression vectors.

RESULTS

Identification of HCNEs in the *Gli3* locus. Previous phylogenetic footprinting studies compared human with fugu intronic *Gli3* sequences and identified a number of highly conserved noncoding elements (1–3, 54). These elements are likely to control *Gli3* expression in domains that are conserved between amniotes and fishes. Indeed, *in vivo* assays showed that some of these HCNEs drive reporter gene expression in conserved sites of expression such as the central nervous system (CNS) (1, 3, 54). The zebrafish *Gli3* temporal expression pattern and its role in the control of spinal cord neuronal differentiation diverge significantly from that of amniote *Gli3* (14, 46, 47, 66), which raised the possibility that searches including amphibian and fish genomes would miss important elements that are critical for the spatiotemporal pattern and thus the function of Gli3 in amniotes. This prompted us to compare the sequence alignments of mammalian, bird, amphibian, and fish *Gli3* sequences and focus our study on 170 kb surrounding the start codon, with the view of including in our study HCNEs conserved in amniotes but not in the teleost and amphibian genomes. In line with other studies (23, 44), a minimum criterion of 60% (for chicken, xenopus frog, and zebrafish) or 65% (for human, rat, and mouse) homology over 100 bp was applied to identify potential HCNEs. This allowed us to identify a total of 19 elements, including 1 HCNE immediately upstream of exon 1, 10 HCNEs in intron 1, and 8 HCNEs in intron 2 (Fig. 1). Comparing our findings with those in previous studies shows that 11 HCNEs, including HCNEs 1 to 3, HCNEs 8 to 12, HCNEs 16 and 17, and HCNE19, were not previously reported (Table 1). In contrast, HCNEs 4 to 7 correspond to HCNR1 as identified by Alvarez-Medina et al. (3), and HCNE5 corresponds to CNE12 as described by Abassi et al. (2). Likewise, HCNEs 13 to 15 correspond to HCNR2 as identified by Alvarez-Medina et al. (3), while HCNEs 13 and 14 correspond to CNE1 as described by Abassi et al. (2). Finally, HCNE18 corresponds to HCNR3 as reported by Alvarez-Medina et al. (3) and to CNE2 as described by Abassi et al. (2).

***In vivo* characterization of HCNE transcriptional activity in the chick neural tube.** To test their putative transcriptional activity, mouse HCNEs were subcloned into a reporter plasmid (nP1230, derived from the plasmid P1230) that contains the β-galactosidase (LacZ) reporter gene under the control of the human β-globin promoter (74) and displays low basal transcriptional activity following *in ovo* electroporation in the chick neural tube (n = 13/38) (see Fig. S1B in the supplemental material). Constructs were coelectroporated with the pMES plasmid, which contains enhanced GFP (EGFP) under the control of the chicken β-actin promoter (63), into the neural tube of HH stage 10 and 11 chicken embryos. LacZ activity was assessed for embryos showing high levels of GFP expression throughout the neural tube after 12 h (at HH stages 13 and 14) (Table 1; see Fig. S1 in the supplemental material) and 24 h (HH stages 15 and 16) (data not shown) of incubation. All regions except four (HCNEs 3 [n = 6], 10 [n = 6], 11 [n = 12], and 12 [n = 8]) showed enhanced transcriptional activity, although five previously reported elements (HCNEs 4 [n = 17/23], 6 [n = 12/20], 13 and 14 [n = 6/9], and 18 [n = 11/11]) and three novel elements (HCNEs 1 [n = 40/53], 2 [n = 10/10], and 9 [n = 13/34]) displayed the strongest increases in LacZ activity compared to that observed in embryos electroporated with nP1230 (see Fig. S1B to D, F, H, K, O, and S in the supplemental material). Interestingly, a number of the putative enhancers tested, including the novel HCNE1 and HCNE9 regions, exhibited a dynamic transcriptional activity along the

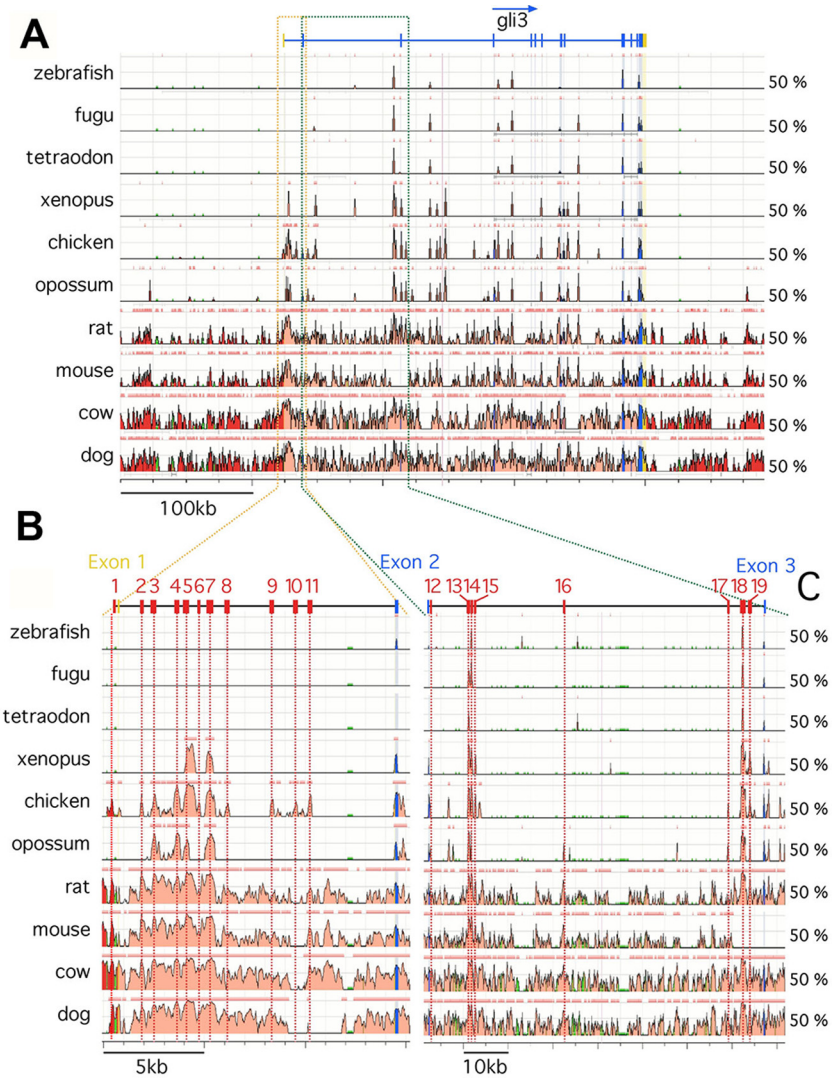

FIG. 1. Sequence comparison of vertebrate Gli3 genomic loci. (A) ECR representations of sequence alignments covering 70 kb upstream of Gli3 exon 2 from human, compared with those for dog, cow, mouse, rat, opossum, chicken, *Xenopus* frog, tetraodon, zebrafish, and fugu. (B) VISTA representations of sequence alignments covering 70 kb between exons 2 and 3 from human, compared with those for dog, cow, mouse, rat, opossum, chicken, *Xenopus* frog, tetraodon, zebrafish, and fugu. Conserved coding regions are indicated in blue, 5′ and 3′ untranslated regions are indicated in yellow, and intronic and exogenic highly conserved noncoding elements (HCNE) are indicated and numbered in pink and red, respectively. HCNEs were defined as having a minimum homology of 60% over 100 bp.

anteroposterior axis of the embryo, with strong expression in the posterior neural tube and dorsally restricted expression in the anterior neural tube (see Fig. S1C, D, M, and K in the supplemental material). At 24 h postelectroporation, this dynamic transcriptional activity persisted and resulted in reporter gene expression detected at high levels in the posterior neural tube and rapidly becoming dorsally restricted at the lumbar axial level (data not shown). This expression pattern was reminiscent of that of endogenous *Gli3*, which is first expressed throughout the neural tube before becoming restricted to a dorsal domain as the neural tube develops (14) (see Fig. S1A in the supplemental material), suggesting that some of these HCNEs may indeed control *Gli3* activation *in vivo*.

HCNE1 is an intronic element in the mouse embryo. The location of HCNE1 immediately upstream of exon 1 suggested that HCNE1 could belong to a promoter element, although predictive tools did not recognize HCNE1 as a putative promoter. Thus, we performed 5′ RACE on E9.5 mouse cDNA, using a primer embedded in exon 3 to determine which transcriptional start site *Gli3* utilizes in mouse embryos. Surprisingly, none of the cDNAs identified contains exon 1 (Fig. 2A). Instead, we find that transcripts expressed in E9.5 mouse embryos include a novel exon, exon 1b, located upstream of exon 1, which contains a consensus 5′ splice donor site and splices directly to exon 2 (Fig. 2A). The transcript generated is consistent with an expressed sequence tag (EST) present in the EBI database (accession no. AK144851) and would not affect the protein product, as the translational start site is located in exon 2. In light of these data, we inferred that HCNE1 is an intragenic element with putative enhancer activity (Fig. 2B).

TABLE 1. HCNEs

Region	Human/chicken alignment		Transcriptional activity[a]	Corresponding region in:		No. of embryos showing Lacz expression/total no. examined
	Length (bp)	% identity		Alvarez-Medina et al. (3)	Abassi et al. (2)	
1	229	61	Strong; DV gradient			40/53
2	132	83.3	Strong; DV gradient			10/10
3	406	68.5	Negative			5/6
4	455	79.8	Strong; continuous	HCNR1; weak expression in neural tube		17/23
5	720	87.4	Moderate; DV gradient	HCNR1; weak expression in neural tube	CNE12; not tested *in vivo*	9/14
6	244	61.5	Strong; DV gradient	HCNR1; weak expression in neural tube		12/20
7	542	79.9	Moderate; AP gradient	HCNR1; weak expression in neural tube		3/9
8	214	64.5	Moderate; DV gradient			6/8
9	226	61.9	Strong; DV gradient			13/34
10	203	80.3	Negative			1/6
11	111	62.2	No activity			11/12
12	355	69	No activity			5/8
13	483	89.6	Strong; DV gradient	HCNR2; strong expression in neural tube	CNE1; anterior CNS in zebrafish	6/9
14	487	90.1	Strong; DV gradient	HCNR2; strong expression in neural tube	CNE1; anterior CNS in zebrafish	6/9
15	229	76.9	Moderate; DV gradient	HCNR2; strong expression in neural tube		10/13
16	271	67.5	Weak; posterior			4/5
17	98	78.6	Weak; dorsal			5/7
18	1,090	93.1	Strong; excluded from floor plate	HCNR3; moderate expression in neural tube	CNE2; anterior CNS in zebrafish and mouse	11/11
19	433	71.1	Weak			3/7

[a] AP, anteroposterior; DV, dorsoventral.

HCNE1 contains TALE protein binding sites that mediate HCNE1 activity along the anteroposterior axis of the neural tube. HCNE1 is of interest because it is uncharacterized, presents a strong transcriptional activity, and drives reporter gene expression with a spatiotemporal pattern similar to that of endogenous *Gli3* (Fig. 2D). Furthermore, HCNE1 displays a high degree of conservation in amniotes but is not conserved in the zebrafish, *Xenopus* frog, or fugu genomes. Mouse HCNE1 is 231 bp long, contains a number of putative binding sites within the first 187 bp, and includes a 78-bp sequence with 86% identity to the human sequence (Fig. 2B). To determine the minimal sequence required for HCNE1 transcriptional activity, we tested various deletion constructs and found that HCNE1-187 displayed similar reporter gene expression upon electroporation in the chick neural tube, as does HCNE1 (Fig. 2D; compare with Fig. S1C in the supplemental material). Predicted binding sites for MyT1 (myeloid transcription factor 1), a zinc finger transcription factor expressed predominantly in the CNS (9), were found at the 5′ extremity of HCNE1-187. Further deletion analyses confirmed that they are not necessary for HCNE1 transcriptional activity, as a 78-bp fragment lacking the MyT1 binding sites was still sufficient to drive β-Gal activity in the neural tube (n = 13/18; data not shown). HCNE1-78, which retains all HCNE1 transcriptional activity, contains two TALE (*t*hree-*a*mino-*a*cid *l*oop *e*xtension) protein binding sites, including site 1, which contains a putative Pbx binding site, and site 2, which contains a compound Meis-Pbx binding site (Fig. 2B and 3A). In addition, it contains putative binding sites for the paired-box transcription factors Pax6 and Pax5, for activating protein 1 (AP-1), and for nuclear factor Y (NFY) (Fig. 2B). However, sequence comparison of the human, mouse, rat, and chick HCNE1-78 elements reveals that binding sites for Pax6, Pax5, and AP-1 are not conserved to the same degree as those for TALE proteins in the chick genome (Fig. 3A), suggesting that TALE proteins may mediate HCNE1 transcriptional activity. The TALE family of transcription factors is composed of the PBC (PBX and CEH-20), Meis, Prep, Iro (Iroquois), Mkx (Mohawk), and Tgif homeodomain transcription factors, although members of the Iro and Mkx gene families are evolutionarily more distant (51). Pbx proteins bind the consensus sequence AATCA (present in site 1) as monomers with low affinity (20) but bind DNA with high affinity as heterodimers with members of the Meis/Prep family or with Hox proteins (12, 18, 19). Meis, Prep, and Tgif homeodomain proteins bind a consensus motif, CTGTCA, which is present at site 2 (13).

To address whether site 1 and site 2 play a role in HCNE1 transcriptional activity, we electroporated wild-type, site 1^{mut}, site 2^{mut}, and site $1/2^{mut}$ reporter constructs in the chick neural tube (Fig. 2C to F). Electroporation of the site 1^{mut} construct does not affect reporter gene expression (n = 21/21; data not shown), whereas a reporter gene construct in which site 2 is mutated causes a consistent reduction of reporter gene activation in the posterior neural tube (n = 15/23) (Fig. 2I; also compare Fig. 2Ei and 2Di), suggesting that TALE protein binding on site 2, but not on site 1, is necessary for HCNE1 transcriptional activity. Interestingly, mutation of site 2 does not affect reporter gene dorsalization in the anterior neural tube (Fig. 2Eii). As the TALE binding site in site 2 can be recognized by any of the three protein families (Meis, Prep, or

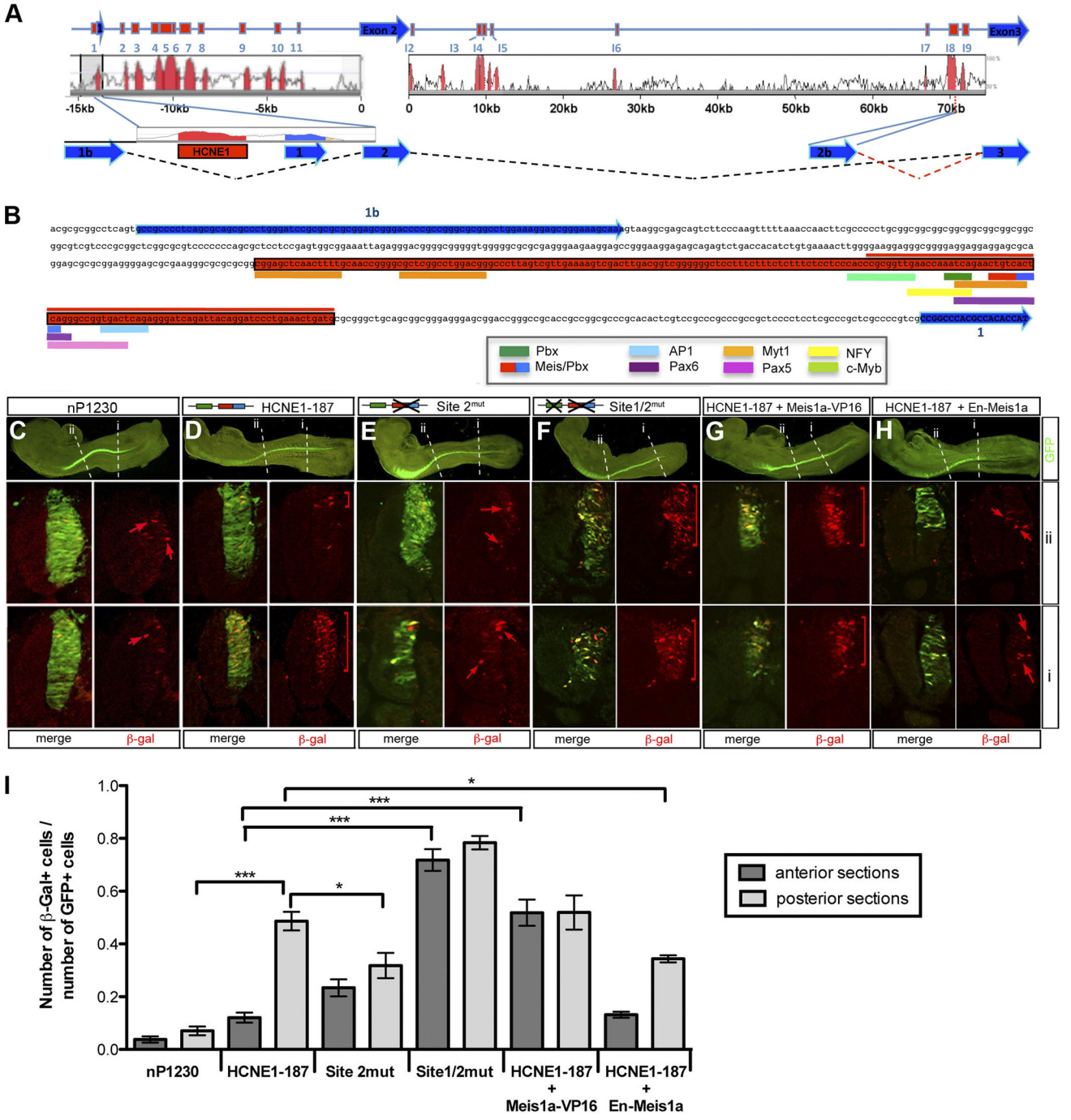

FIG. 2. HCNE1 is an intronic element with transcriptional activity in the chick neural tube. (A) Schematic representation of the various 5′ RACE products identified from mouse embryo cDNAs in relation to the 5′ end of the *Gli3* genomic locus as reported in Ensembl and the different HCNEs identified. (B) Sequence of the genomic region between exons 1 and 1b. Exons are indicated in blue and HCNE1 in red. Predicted transcription factor binding sites found in mouse HCNE1 are shown with colored thick lines below the HCNE1 sequence. HCNE1-78, which lacks all Myt1 binding sites, is indicated by a red line above the sequence. Site 1, which contains a Pbx binding site, is indicated in green, and site 2, which contains a compound Meis/Pbx binding site, is indicated in red/blue. (C to H) β-Galactosidase (β-Gal) protein expression following *in ovo* electroporation in the chick neural tube of nP1230 (C), HCNE1-187 (D), site 2^{mut} (E), site $1/2^{mut}$ (F), HCNE1-187 with Meis1a-VP16 (G), and HCNE1-187 with En-Meis1a (H). Coelectroporation with a control GFP plasmid served as an internal control (left panels). β-Gal expression was examined by immunofluorescence on cryosections at the anterior and posterior axial levels as indicated by "i" and "ii." Note that electroporation of HCNE1-187 results in strong β-Gal expression (D) compared to the level for nP1230 (C), with an anteroposterior pattern reminiscent of *Gli3* expression. Mutations in site 2 (E) or coelectroporation with a Meis1a-En construct (H) reduces HCNE1-187 activity, whereas mutations is both site 1 and site 2 (F) or coelectroporation with a Meis1a-VP16 construct (G) impairs HCNE1-187-controlled anteroposterior patterning and results in continuous reporter activity along the axis. Brackets and arrows indicate the domain of β-Gal expression. Magnification is ×25 (left panels) and ×400 (sections). (I) Quantification of HCNE1 *in vivo* transcriptional activity in the anterior and posterior neural tube. The ratio of the number of β-Gal-positive cells over the number of GFP-positive cells per section was plotted for each electroporation condition. Error bars indicate the standard error of the mean. Statistical significance is indicated above the bars and was evaluated using *t* test analysis.

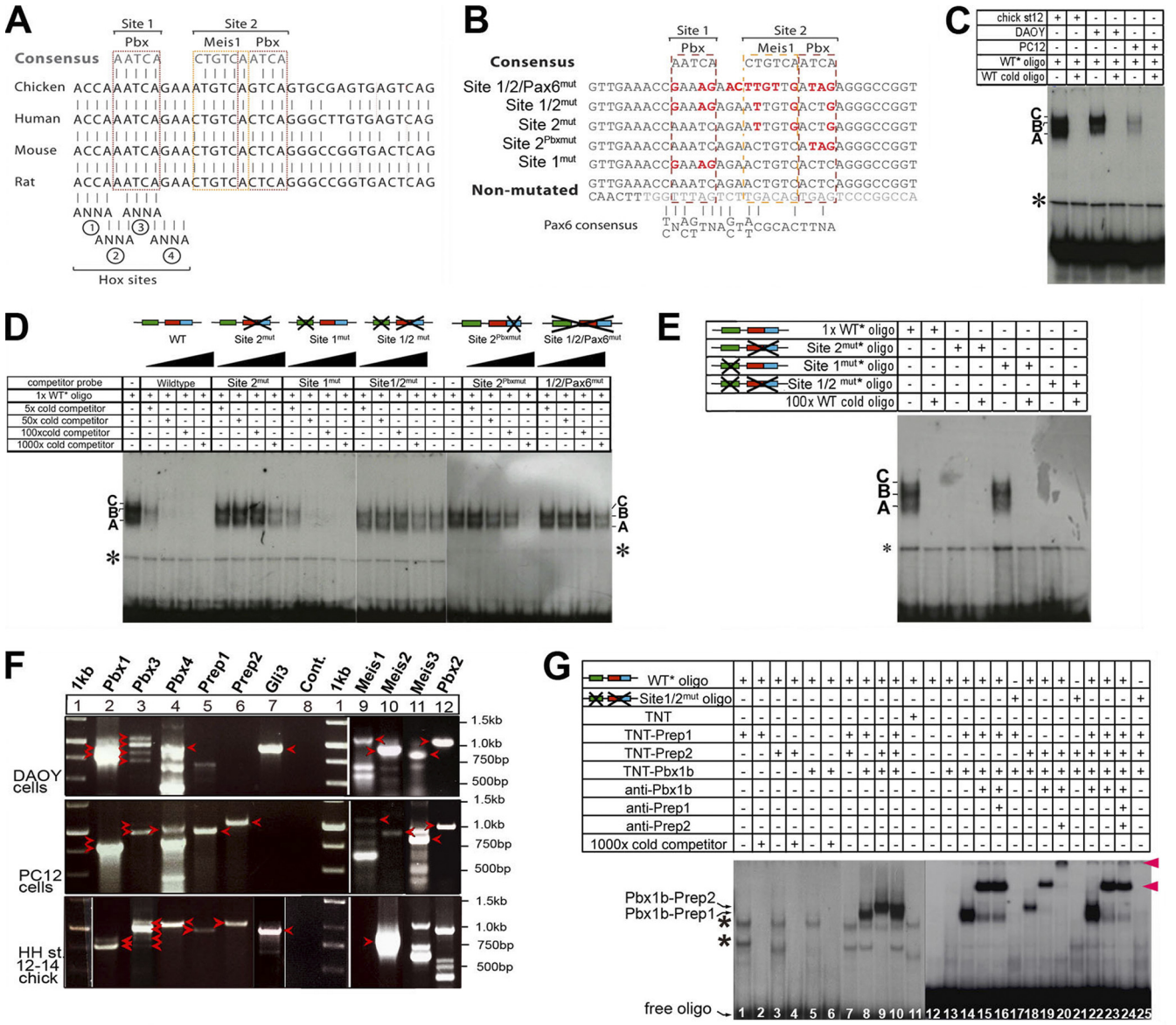

FIG. 3. TALE proteins bind to HCNE1. (A) Sequence alignments of human, mouse, chicken, and rat genomic DNA show a high degree of conservation at sites 1 and 2, which contain binding sites for Pbx and Meis-Pbx, respectively. Four putative Hox binding site core sequences are also indicated, although no Pbx-Hox compound site was identified in databases. (B) Sequence of wild-type and mutated constructs and oligonucleotides used in EMSA and electroporation studies. Mutated nucleotides are indicated in red. (C) EMSA using a 35-bp oligonucleotide containing site 1 and site 2 incubated with nuclear extracts from chicken embryos and DAOY and PC12 cells in the presence/absence of a 1,000-fold excess of cold oligonucleotide. The asterisk indicates nonspecific binding. Complexes are labeled A, B, and C. (D) EMSA using a 35-bp oligonucleotide containing site 1 and site 2 incubated with nuclear extracts from chicken embryos in the presence of increasing amounts (5-, 50-, 100-, and 1,000-fold) of cold wild-type or mutated oligonucleotides. (E) EMSA using a 35-bp oligonucleotide containing no mutation or mutations in site 1, site 2, or sites 1 and 2 incubated with nuclear extracts from chicken embryos in the presence or absence of a 100-fold excess of cold wild-type oligonucleotide. (F) Expression of Pbx, Meis, and Prep genes was assessed using RT-PCR on mRNA extracted from DAOY cells, PC12 cells, and chicken embryos. Loading and expected sizes are as follows: lane 1, 1-kb DNA ladder; lane 2, 901 bp (Pbx1a) and 788 bp (Pbx1b); lane 3, 1,073 bp (Pbx3a), 960 bp (Pbx3b), 831 bp (Pbx3c), and 718 bp (Pbx3d); lane 4, 983 bp (Pbx4); lane 5, 959 bp (Prep1); lane 6, 1,059 bp (Prep2); lane 7, 929 bp (Gli3); lane 8, negative control; lane 9, 1,156 bp (Meis1a); lane 10, 934 bp (Meis2a); lane 11, 766 bp (Meis3); lane 12, 1,146 bp (Pbx2). Bands observed at the expected sizes and confirmed through sequencing are indicated with arrowheads. The other PCR products observed either are nonspecific bands or upon sequencing were found to be a paralogue (as is the case for the RT-PCR bands present in lane 12 that proved to not contain *Pbx2* upon sequencing). Arrowheads indicate bands at the expected sizes. (G) EMSA using a 35-bp oligonucleotide containing either wild-type site 1 and site 2 or mutated site 1 and site 2 that was radiolabeled and incubated with *in vitro*-translated Pbx1b, Prep1, and Prep2 proteins in the presence or absence of anti-Pbx1b, anti-Prep1, or anti-Prep2 antisera. Asterisks indicate nonspecific binding bands.

Tgif), we used constitutively active or repressive Meis constructs to assess whether binding of a TALE protein could affect HCNE1 transcriptional activity. Coelectroporation of wild-type HCNE1-187 with an En-Meis1a construct that acts in a dominant-negative manner (75) causes a downregulation of reporter gene expression similar to that caused by mutations in site 2 ($n = 15/20$) (Fig. 2I; also compare Fig. 2H and 2D). In contrast, coelectroporation of a Meis1a-VP16 ($n = 26/29$) construct with HCNE1-187 has little or no effect on reporter gene activation in the posterior neural tube but interferes with the normal dorsalization of reporter gene expression in the anterior neural tube (Fig. 2I; also compare Fig. 2Gii and 2Dii). Together, these data suggest that TALE proteins positively regulate HCNE1 transcriptional activity through their binding to site 2. Our results also imply that dorsalization of reporter gene expression in the anterior neural tube is the consequence of either the exhaustion of TALE proteins or the inactivity of TALE proteins in the anterior neural tube, as ectopic expression of a constitutively active TALE protein is sufficient to maintain high levels of HCNE1 activity in the anterior neural tube. Thus, site 2 is required for HCNE1 activity, and levels of TALE protein activity are likely to affect the transcriptional output from HCNE1. Together with our recent findings that TALE genes are dynamically expressed during neural development (see Fig. 6A) (25), these data are consistent with the hypothesis that TALE proteins control how HCNE1-mediated expression is patterned along the anteroposterior axis of the neural tube.

Surprisingly, we observe that mutation of both site 1 and site 2 ($n = 9/13$) does not eradicate reporter gene expression but results in the maintenance of reporter gene expression in the anterior neural tube (Fig. 2F). We ruled out the possibility that mutations in sites 1 and 2 do not completely eliminate site 1/2, as radiolabeled site $1/2^{mut}$ oligonucleotides fail to bind Pbx1b and Prep1 or Prep2 in an electrophoretic mobility shift assay (EMSA) (Fig. 3G). Thus, possible explanations for this somewhat contradicting result are either the creation of new putative binding sites in the site $1/2^{mut}$ construct or the unmasking and serendipitous activity of additional binding sites in HCNE1-187 that do not encompass the region of our EMSA oligonucleotides in the absence of TALE complexes. Consistent with the former possibility, longer exposure of an EMSA autoradiography using radiolabeled site 2^{mut} and site $1/2^{mut}$ oligonucleotides confirms the existence of additional faint complexes (see Fig. S2 in the supplemental material).

TALE protein heterodimers bind cooperatively to HCNE1 *in vitro*. To test whether TALE protein members bind to HCNE1, we performed EMSAs using a 36-bp radioactively labeled oligonucleotide encompassing both site 1 and site 2 (Fig. 3B). Three specific complexes (termed A, B, and C) form in the presence of nuclear extract from HH stage 12 to 14 chick embryos, whereas two complexes form in the presence of nuclear extract from DAOY medulloblastoma cells that express *Gli3* (Fig. 3F, lane 7) and are competed by an excess of unlabeled oligonucleotide (Fig. 3C). In contrast, we observe a weak formation of complexes in the presence of nuclear extract from PC12 neuronal cells (Fig. 3C) that do not express *Gli3* (Fig. 3F, lane 7). To address whether complexes A, B, and C form on site 1 or site 2, we assessed the ability of various mutant oligonucleotides (shown in Fig. 3B) to compete with radiolabeled wild-type oligonucleotides for the formation of complexes in the presence of embryonic nuclear extract (Fig. 3D). Our data show that site 1^{mut} oligonucleotides compete as efficiently as wild-type oligonucleotides, indicating that the upstream Pbx binding site is dispensable for the formation of complexes A, B, and C (Fig. 3D). In contrast, all other mutated oligonucleotides displayed little (site 2^{Pbxmut}) or no (site 2^{mut}, site $1/2^{mut}$, and site $1/2/Pax6^{mut}$) competition with the wild-type radiolabeled oligonucleotide, suggesting that complexes form on site 2 (Fig. 3D). Moreover, competition was greatly affected by site 2^{Pbxmut} oligonucleotides in which the Pbx, but not the Meis binding site of site 2, is mutated (Fig. 3B), suggesting that Pbx proteins may be an important component of complexes A, B, and C. Consistent with these observations, radiolabeled site 1^{mut} oligonucleotides form three complexes in the presence of chicken embryo nuclear extracts, and these complexes can be competed with unlabeled wild-type oligonucleotides (Fig. 3E). In contrast, neither site 2^{mut} nor site $1/2^{mut}$ radiolabeled oligonucleotides are able to form a complex with nuclear proteins (Fig. 3E), confirming that mutations in site 2 disrupt its interaction with nuclear proteins.

We next performed RT-PCR assays to establish which members of the TALE gene family were expressed in DAOY cells, PC12 cells, and HH stage 12 to 14 chick embryos using specific primers that detect multiple isoforms of *Pbx*, *Meis*, and *Prep* genes (data available on request). All PCR products were sequenced to confirm that the correct gene family member had been amplified. Interestingly, DAOY cells, which express *Gli3*, contain all *Pbx* and *Meis* transcripts but do not express *Prep1* or *Prep2* (Fig. 3F, lanes 1 to 6 and 9 to 12). In contrast, both *Prep1* and *Prep2* are present in PC12 cells (Fig. 3F, lanes 5 and 6), while PC12 cells lack *Pbx1a*, *Pbx3c*, and *Pbx3d* (Fig. 3F, lanes 2 and 3) and express *Meis* genes at low levels (Fig. 3F, lanes 9 to 11). In HH stage 12 chick embryos, we found that *Pbx1b*, *Pbx3b*, and *Pbx4* were the predominant *Pbx* isoforms present but could not amplify *Pbx2* (Fig. 3F, lanes 1 to 4). HH stage 12 chick embryos also express *Meis1*, *Meis2*, *Prep1*, *Prep2*, *Tgif1*, and *Tgif2* but not *Meis3* (Fig. 3F) (25). As the CTGTCA core in site 2 can bind members of the Meis, Prep, or Tgif families and both Meis and Prep proteins can form heterodimers with Pbx proteins, we tested whether *in vitro*-translated Pbx1b, Prep1, and Prep2 bind to radiolabeled wild-type oligonucleotides. No binding was observed in the presence of monomers of Pbx1b, Prep1, and Prep2 alone or in the presence of Prep1 and Prep2 together (Fig. 3G, lanes 1 to 7). However, cooperative binding was observed when Pbx1b was combined with Prep1, Prep2, or both (Fig. 3G, lanes 8 to 10, 14, 18, and 22), indicating that Pbx1b binds HCNE1 as heterodimers of Pbx1b-Prep1 or Pbx1b-Prep2. This binding was specific, as no complex formed on radiolabeled site $1/2^{mut}$ oligonucleotides (Fig. 3G, lanes 17, 21, and 25). Furthermore, Pbx1b-Prep1 and Pbx1b-Prep2 complexes migrated with an electromobility similar to that of complexes A and B observed in the presence of embryo extract (data not shown), suggesting that Pbx1b forms different heterodimeric complexes with Prep proteins *in vivo*. Finally, antibodies directed against Pbx1b and Prep2 caused a supershift or super-supershift of Pbx1b-Prep1 and Pbx1b-Prep2 complexes (indicated by red arrowheads in Fig. 3G, lanes 15, 16, 19, 20, 23, and 24), while anti-Prep1 antibodies

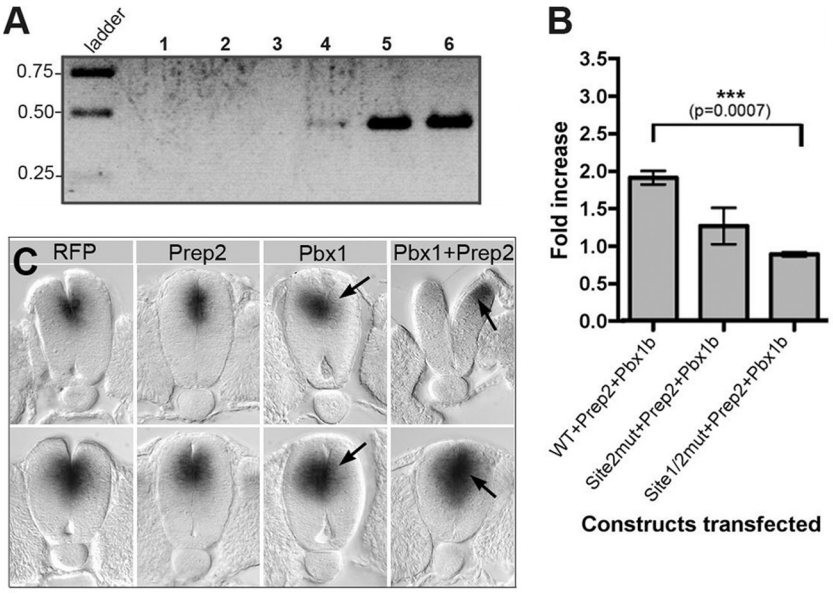

FIG. 4. Pbx-containing heterodimers bind to and transactivate HCNE1 *in vivo*. (A) A chromatin immunoprecipitation (ChIP) assay was performed on E9.5 mouse embryos by use of antibodies against β-Gal (lane 3), Meis (lane 4), or Pbx (lane 5). Immunoprecipitated DNA was amplified by semiquantitative PCR. Lane 1, negative PCR control containing no DNA; lane 2, ChIP protocol performed with no antibody; lane 6, input chromatin (one-third less product was loaded on the gel). (B) HCNE1 transcriptional activity is enhanced by Pbx1b and Prep2. HeLa cells were cotransfected with a wild-type, site 2^{mut}, or site $1/2^{mut}$ HCNE1 reporter construct in the presence or absence of equal amounts of the Pbx1b and Prep2 expression constructs. The fold increase of relative luciferase activity was measured as the ratio of HCNE1-dependent luciferase activity normalized to the level for *Renilla* luciferase obtained in the presence of Pbx1b and Prep2, compared to that obtained in the absence of Pbx1b and Prep2. (C) Effect of Pbx1b and Prep2 on endogenous *Gli3* expression. Prep2, Pbx1b, or Prep2+Pbx1b expression constructs were coelectroporated with a RFP plasmid in the chick neural tube, and effect on *Gli3* expression was assayed by whole-mount *in situ* hybridization, followed by Vibratome sectioning. Whole-mount photographs of RFP and *Gli3* expression are shown in Fig. S3 in the supplemental material. Top panels show caudal transverse sections, whereas bottom panels show rostral transverse sections along the neural tube. Arrows indicate up- or downregulation on the electroporated side (right). Note that the top panel for Pbx1+Prep2 electroporation shows a more posterior section to illustrate the precocious activation of *Gli3* in these embryos. At this axial level, *Gli3* would normally not be activated yet (or at very low level), as attested by expression on the nonelectroporated side.

appeared unable to shift Pbx1b-Prep1 complexes, possibly because the epitope was masked. Together, these data indicate that Pbx proteins bind site 2 as heterodimers with Prep proteins.

Consistent with these data, chromatin immunoprecipitation (ChIP) analyses of E9.5 mouse embryos show a specific amplification of a DNA fragment containing site 1 and site 2 with anti-Pbx antibodies (Fig. 4A, lane 5) and to a lesser extent with anti-Meis antibodies (Fig. 4A, lane 4) but not with control anti-β-Gal antibodies (Fig. 4A, lane 3). Furthermore, cotransfection of HeLa cells with expression vectors coding for Pbx1b and Prep2 causes a 2-fold increase in reporter gene activity compared with the level for cells transfected with the HCNE1 reporter construct alone (Fig. 4B). Mutations in site 2 or in both site 1 and site 2 significantly reduce the transcriptional activity of the HCNE1 reporter construct in the presence of Pbx1b and Prep2 (Fig. 4B), confirming that Pbx and Prep proteins can synergistically enhance HCNE1 activity. Finally, although electroporation of a red fluorescent protein (RFP; $n = 2$) expression construct or a *Prep2* ($n = 3$) expression construct alone in the chick neural tube has no effect on endogenous *Gli3* expression, we found that ectopic expression of *Pbx1* together with *Prep2* caused precocious and increased expression of *Gli3* in the dorsal neural tube ($n = 4/6$) (Fig. 4C). Interestingly, ectopic expression of *Pbx1* alone had a converse effect and led to a decrease in *Gli3* activation ($n = 4/5$) (Fig. 4C), suggesting that in the absence of heterodimer formation with a member of the Meis/Prep protein family, Pbx1 may associate with repressor factors that impact negatively on *Gli3* transcription.

Loss of Pbx1 affects *Gli3* expression levels in the developing neural tube of the mouse embryo. To further establish whether binding of Pbx protein to HCNE1 plays a role in *Gli3* regulation *in vivo*, we examined E10.5 mouse embryos with a targeted mutation in the *Pbx1* locus (62). Although the overall expression of *Gli3* appeared unaffected in $Pbx1^{-/-}$ embryos (data not shown), we observed that *Gli3* expression was strongly upregulated in the posterior neural tube and expressed in the floor plate, where it is normally excluded (Fig. 5). Together with our previous observation that ectopic expression of Pbx1 downregulates *Gli3* expression in the chick neural tube, this result suggests that levels of Pbx1 and the absence or presence of Meis/Prep proteins are critical for the regulation of *Gli3* transcriptional output. Remarkably, loss of *Pbx1* affected *Gli3* expression only in the posterior neural tube, suggesting the existence of compensatory roles of other *Pbx* genes elsewhere in the embryo (16, 17). Indeed, previous studies showed that the *Gli3* expression domain expands in $Pbx1^{-/-}$; $Pbx2^{+/-}$ limbs (16), although, in this case, it has been suggested that *Gli3* expansion occurs as a consequence of Shh downregulation.

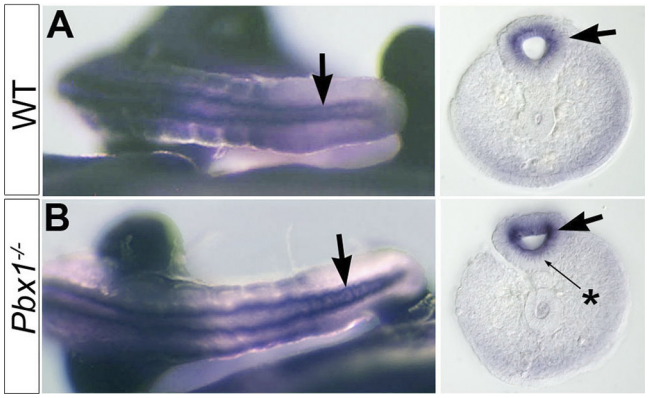

FIG. 5. *Gli3* is upregulated in the rostral neural tube of *Pbx1*$^{-/-}$ embryos. Tail *Gli3* expression is detected by whole-mount *in situ* hybridization of E10.5 wild-type (A) and *Pbx1*$^{-/-}$ (B) mouse embryos, followed by Vibratome sectioning (right panels). Arrows indicate *Gli3* upregulation in the neural tube. Note *Gli3* transcripts in the floor plate (star) in the absence of *Pbx1*.

DISCUSSION

Gli3 is an essential transcription factor that antagonizes or mediates Shh signaling in a context-dependent manner during embryogenesis. Thus, Gli3 expression is highly regulated both temporally and spatially, and disruption in this expression pattern is often associated with developmental defects. To gain insight into the mechanisms that control *Gli3* expression, we have used phylogenetic footprinting to identify a highly conserved noncoding element (HCNE1) located immediately upstream of *Gli3* exon 1. This element is distinct from highly conserved noncoding elements previously identified by others (1–3, 54). We show here that HCNE1 contains a compound Meis-Pbx binding site, bound *in vitro* and *in vivo* by members of the Pbx and Meis/Prep protein families. Mutations in this Meis-Pbx binding site cause loss of reporter gene expression, while ectopic expression of Pbx and Meis/Prep causes precocious and prolonged expression of *Gli3* and the reporter gene. Together, our data suggest that Pbx and Meis/Prep proteins may play an essential role in the control of the Shh response by regulating the transcription levels of *Gli3* through their specific association with cofactors. This observation provides an attractive model for fine-tuning the spatiotemporal control of *Gli3* expression during embryogenesis.

We show that Pbx1b associates with Prep1 and Prep2 and to a lesser extent with Meis proteins and that, together, these proteins induce HCNE1 transcriptional activity and *Gli3* expression. As *Prep1* and *Prep2* are differentially expressed along the anteroposterior and dorsoventral axes of the neural tube (Fig. 6A) (25), we propose that Pbx1b/Prep1 complexes control the initiation of *Gli3* expression and that Pbx1b/Prep2 complexes are involved at the time *Gli3* becomes dorsalized (Fig. 6B). Moreover, as overexpression of Pbx1b alone in the chick neural tube or loss of Pbx1 function in the mouse embryo elicits repression or ventral expansion of *Gli3* expression, respectively, we propose that binding of Prep proteins to Pbx1b displaces and competes with the binding of a repressor to Pbx1b (Fig. 6B). Thus, complexes forming on HCNE1 are dynamic, and competitive cooperative binding between activators or repressors and Pbx1 on HCNE1 is likely to yield different transcriptional outputs. This model could provide a molecular basis for our observation that reporter gene expression mediated by HCNE1 presents a pattern similar to that presented by *Gli3* and that manipulation of Pbx1b and Prep protein levels has a differential effect on *Gli3* expression.

Our study has essentially focused on the interaction of Pbx1b with Prep1 or Prep2. However, other TALE proteins could be involved in HCNE1 activity. Our RT-PCR data reveal that in addition to *Pbx1b*, *Pbx3b* and *Pbx4* are also abundantly expressed in HH stage 12 to 14 chick embryos, although *Pbx3* is not expressed in the neural tube (Fig. 3F) (25). This indicates that the most likely candidate for binding of the Pbx half-site of site 2 is Pbx1, Pbx4, or both. What are the partners of Pbx in *Gli3* regulation? Our data point to the existence of heterodi-

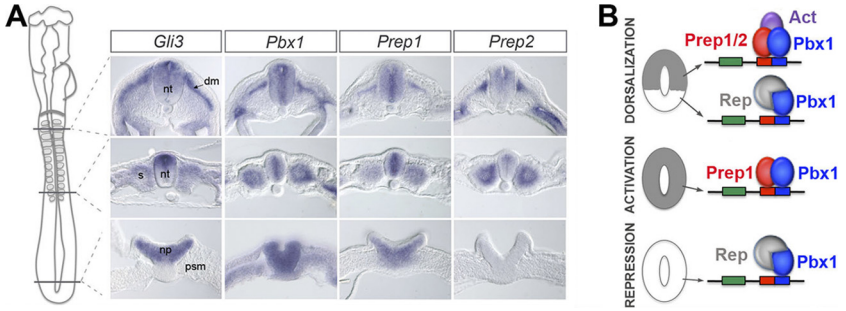

FIG. 6. Model for the control of HCNE1 transcriptional activity and *Gli3* expression by TALE proteins. (A) Expression pattern of *Gli3*, *Pbx1*, *Prep1*, and *Prep2* in HH stage 12 chick embryos. Transverse sections shown correspond to the axial level indicated on the cartoon (left). psm, presomitic mesoderm; np, neural plate; nt, neural tube; s, somite; dm, dermomyotome. Note *Gli3* and *Pbx*/*Prep* overlapping expression domains in the developing neural tube and somites. Note that the posterior-most section of *Pbx1* is slightly more posterior than indicated while that of *Prep2* is slightly more anterior than indicated. (B) Working model for *Gli3* control in the neural tube. We propose that distinct complexes form on HCNE1 along the anteroposterior axis and that availability of Prep (or Meis) proteins dictates the steady state of HCNE1 complexes. We hypothesize that in its inactive state, HCNE1 is bound by Pbx1b (or Pbx4) associated with a repressor. Prep and Meis proteins can displace this complex, and thus, as *Prep1* is broadly expressed in the posterior neural plate, *Prep1* associates with Pbx1b (or Pbx4) at site 2 to induce *Gli3* expression. As neurogenesis proceeds, *Gli3* becomes dorsally restricted in the anterior neural tube. This may be triggered by the formation of new heterodimeric complexes between Pbx1 (or Pbx4) and Prep2 (or members of the Meis gene family) and could be aided by the formation of heterotrimeric complexes with other transcriptional activators (Act). In addition, we propose that repression of *Gli3* transcription in the ventral neural tube is mediated/reinforced via the specific interaction of Pbx with a repressor (Rep).

meric and perhaps heterotrimeric complexes forming on site 2, and we have shown that Pbx1b-Prep1 and Pbx1b-Prep2 heterodimeric complexes have mobilities similar to those of embryonic complexes A and B, respectively. However, our data also show that a Meis protein is weakly bound *in vivo* to HCNE1, and our previous expression analysis of *Tgif* genes suggest that they may also be candidate proteins for association with Pbx proteins on HCNE1 (25). In support of the possible involvement of Tgif is the fact that ectopic *Tgif1* expression in the chick neural tube causes a downregulation of dorsal neural tube markers similar to that caused by ectopic *Gli3* expression (38, 56). Furthermore, mutations in human and mouse *Tgif* disrupt the dorsoventral patterning of the neural tube and cause holoprosencephaly, a phenotype initially attributed to aberrant retinoic acid signaling (27, 29, 39), although our data could suggest a connection with loss of Shh signaling. Thus, various Pbx-Meis, Pbx-Prep, and Pbx-Tgif heterodimeric complexes could form on site 2. This is of importance, as previous studies have shown that different Pbx paralogues have distinct affinities for partner proteins. For instance, Pbx1, but not Pbx2 or Pbx3, is unable to bind DNA alone and requires association with a Meis/Prep partner (53). In addition, Pbx splice variants can have opposing transcriptional activities. One example of this is Pbx1, whose "b" isoforms can form complexes that activate transcription (5, 28), whereas Pbx1a can inhibit transcription through its association with histone deacetylase (HDAC) proteins and the corepressors NcoR and SMRT (5, 60). The ability of Pbx1, as well as Tgif, to interact with the chromatin remodeling protein HDAC to generate repressive complexes provides a possible mechanism for our proposed inhibition of *Gli3* in the absence of Prep proteins (8, 10, 60). Such mechanism has already been reported for Hoxb-controlled genes (22). Further studies are required to establish whether such interaction exists on HCNE1 and participates in the control of *Gli3* expression.

Pbx proteins can also form heterotrimeric complexes containing a member of the Meis protein family and another transcriptional regulator, as in the case of the myogenin promoter for which binding of Pbx-Meis is required for subsequent activation by MyoD and recruitment of the SWI/SNF chromatin remodeling complex (10, 11). The presence of higher-molecular-weight complexes in EMSAs (complex C) attests to the possibility that heterotrimeric complexes form on site 2. This is a very attractive possibility that would allow integration of multiple outputs from distinct signaling pathways toward the transcriptional control of *Gli3* expression. For instance, BMP signaling is required for *Gli3* maintenance in the neural tube (49). Smads, the transcriptional effectors of BMP signaling, can bind Pbx1-Prep1 and Pbx1-Tgif complexes (8, 73). As BMP signaling is restricted to the dorsal neural tube, Pbx1-Prep1-Smad heterotrimeric complexes could thus participate in the maintenance of *Gli3* in the dorsal spinal cord. Future studies will be required to identify whether other transcription factors, such as Smads, are implicated in heterotrimeric complexes on HCNE1.

While HCNE1 in isolation is sufficient to faithfully mimic the *Gli3* expression pattern, in the context of the whole locus *Gli3* expression is presumably governed by the combinatorial effects of multiple HCNEs. Indeed, other studies have reported additional elements implicated in the control of *Gli3* expression in the CNS (1–3, 54). Interestingly, computing analyses reveals that CNE13-14 (HCNRE2 in reference 3), which also displays strong transcriptional activity in the neural tube, contains two conserved Pbx binding sites, suggesting a mechanism whereby TALE proteins could globally regulate the transcription of *Gli3* via multiple binding sites spread over several CNEs. Such regulation may also apply to other sites of *Gli3* expression. Indeed, there is a striking overlap between the expression domains of *Gli3* and that of *Pbx1*, *Prep1*, and *Prep2* in the paraxial mesoderm (Fig. 6A). Further studies will establish whether HCNE1 plays a role in mesodermal *Gli3* expression.

ACKNOWLEDGMENTS

We are grateful to A. Furley and J. Weiss for providing us PC12 and DAOY cell lines, to E. Smythe for providing us with the pcDNA3 expression vector, to M. Torres for providing us with cMeis1 and cMeis2 plasmids, and to R. Maas for providing us with En-Meis1a and Meis1a-VP16 constructs. We thank C. Nicolas for technical support and Jeremy Sanderson at the Sheffield Light Microscopy facility for his technical assistance. We thank A. Furley and A. Brendolan for their critical reading of the manuscript and suggestions.

This work was supported by grants from the EU-FP6 program (Cells into Organs contract LSHM-CT-2003-504468 and MYORES contract 511978), by the BBSRC (grant number 50/G16004) to A.-G.B., and by grants from the EU-FP6 program MYORES (contract 511978) and the MRC (contract G0401199) to J.C. S.C. was funded by a BBSRC Ph.D. fellowship and by the EU-FP6 grants. The Sheffield Light Microscopy facility was funded by a grant from the Wellcome Trust (grant number GR077544AIA).

REFERENCES

1. **Abbasi, A. A., et al.** 2010. Human intronic enhancers control distinct subdomains of Gli3 expression during mouse CNS and limb development. BMC Dev. Biol. **10:**44.
2. **Abbasi, A. A., et al.** 2007. Human GLI3 intragenic conserved non-coding sequences are tissue-specific enhancers. PLoS One **2:**e366.
3. **Alvarez-Medina, R., J. Cayuso, T. Okubo, S. Takada, and E. Marti.** 2008. Wnt canonical pathway restricts graded Shh/Gli patterning activity through the regulation of Gli3 expression. Development **135:**237–247.
4. **Anderson, C., S. J. Winder, and A. G. Borycki.** 2007. Dystroglycan protein distribution coincides with basement membranes and muscle differentiation during mouse embryogenesis. Dev. Dyn. **236:**2627–2635.
5. **Asahara, H., S. Dutta, H. Y. Kao, R. M. Evans, and M. Montminy.** 1999. Pbx-Hox heterodimers recruit coactivator-corepressor complexes in an isoform-specific manner. Mol. Cell. Biol. **19:**8219–8225.
6. **Aza-Blanc, P., H. Y. Lin, A. Ruiz i Altaba, and T. B. Kornberg.** 2000. Expression of the vertebrate Gli proteins in Drosophila reveals a distribution of activator and repressor activities. Development **127:**4293–4301.
7. **Bai, C. B., D. Stephen, and A. L. Joyner.** 2004. All mouse ventral spinal cord patterning by hedgehog is Gli dependent and involves an activator function of Gli3. Dev. Cell **6:**103–115.
8. **Bailey, J. S., N. Rave-Harel, S. M. McGillivray, D. Coss, and P. L. Mellon.** 2004. Activin regulation of the follicle-stimulating hormone beta-subunit gene involves Smads and the TALE homeodomain proteins Pbx1 and Prep1. Mol. Endocrinol. **18:**1158–1170.
9. **Bellefroid, E. J., et al.** 1996. X-MyT1, a Xenopus C2HC-type zinc finger protein with a regulatory function in neuronal differentiation. Cell **87:**1191–1202.
10. **Berkes, C. A., et al.** 2004. Pbx marks genes for activation by MyoD indicating a role for a homeodomain protein in establishing myogenic potential. Mol. Cell **14:**465–477.
11. **Berthelsen, J., C. Kilstrup-Nielsen, F. Blasi, F. Mavilio, and V. Zappavigna.** 1999. The subcellular localization of PBX1 and EXD proteins depends on nuclear import and export signals and is modulated by association with PREP1 and HTH. Genes Dev. **13:**946–953.
12. **Berthelsen, J., V. Zappavigna, F. Mavilio, and F. Blasi.** 1998. Prep1, a novel functional partner of Pbx proteins. EMBO J. **17:**1423–1433.
13. **Bertolino, E., B. Reimund, D. Wildt-Perinic, and R. G. Clerc.** 1995. A novel homeobox protein which recognizes a TGT core and functionally interferes with a retinoid-responsive motif. J. Biol. Chem. **270:**31178–31188.
14. **Borycki, A., A. M. Brown, and C. P. Emerson, Jr.** 2000. Shh and Wnt signaling pathways converge to control Gli gene activation in avian somites. Development **127:**2075–2087.
15. **Bray, N., I. Dubchak, and L. Pachter.** 2003. AVID: a global alignment program. Genome Res. **13:**97–102.
16. **Capellini, T. D., et al.** 2006. Pbx1/Pbx2 requirement for distal limb patterning

is mediated by the hierarchical control of Hox gene spatial distribution and Shh expression. Development **133:**2263–2273.
17. **Capellini, T. D., et al.** 2008. Pbx1/Pbx2 govern axial skeletal development by controlling Polycomb and Hox in mesoderm and Pax1/Pax9 in sclerotome. Dev. Biol. **321:**500–514.
18. **Chang, C. P., L. Brocchieri, W. F. Shen, C. Largman, and M. L. Cleary.** 1996. Pbx modulation of Hox homeodomain amino-terminal arms establishes different DNA-binding specificities across the Hox locus. Mol. Cell. Biol. **16:** 1734–1745.
19. **Chang, C. P., et al.** 1997. Meis proteins are major in vivo DNA binding partners for wild-type but not chimeric Pbx proteins. Mol. Cell. Biol. **17:** 5679–5687.
20. **Chang, C. P., et al.** 1995. Pbx proteins display hexapeptide-dependent cooperative DNA binding with a subset of Hox proteins. Genes Dev. **9:**663–674.
21. **Chen, Y. X., C. E. Krull, and L. W. Reneker.** 2004. Targeted gene expression in the chicken eye by in ovo electroporation. Mol. Vis. **10:**874–883.
22. **Choe, S. K., P. Lu, M. Nakamura, J. Lee, and C. G. Sagerstrom.** 2009. Meis cofactors control HDAC and CBP accessibility at Hox-regulated promoters during zebrafish embryogenesis. Dev. Cell **17:**561–567.
23. **Cooper, G. M., and A. Sidow.** 2003. Genomic regulatory regions: insights from comparative sequence analysis. Curr. Opin. Genet. Dev. **13:**604–610.
24. **Couronne, O., et al.** 2003. Strategies and tools for whole-genome alignments. Genome Res. **13:**73–80.
25. **Coy, S. E., and A. G. Borycki.** 2010. Expression analysis of TALE family transcription factors during avian development. Dev. Dyn. **239:**1234–1245.
26. **Dai, P., et al.** 1999. Sonic hedgehog-induced activation of the Gli1 promoter is mediated by GLI3. J. Biol. Chem. **274:**8143–8152.
27. **Gongal, P. A., and A. J. Waskiewicz.** 2008. Zebrafish model of holoprosencephaly demonstrates a key role for TGIF in regulating retinoic acid metabolism. Hum. Mol. Genet. **17:**525–538.
28. **Goudet, G., S. Delhalle, F. Biemar, J. A. Martial, and B. Peers.** 1999. Functional and cooperative interactions between the homeodomain PDX1, Pbx, and Prep1 factors on the somatostatin promoter. J. Biol. Chem. **274:** 4067–4073.
29. **Gripp, K. W., et al.** 2000. Mutations in TGIF cause holoprosencephaly and link NODAL signalling to human neural axis determination. Nat. Genet. **25:**205–208.
30. **Hamburger, V., and H. L. Hamilton.** 1951. A series of normal stages in the development of the chick embryo. J. Morphol. **88:**49–92.
31. **Hatzis, P., and I. Talianidis.** 2002. Dynamics of enhancer-promoter communication during differentiation-induced gene activation. Mol. Cell **10:**1467–1477.
32. **Hubbard, T. J., et al.** 2007. Ensembl 2007. Nucleic Acids Res. **35:**D610–D617.
33. **Jacob, J., and J. Briscoe.** 2003. Gli proteins and the control of spinal-cord patterning. EMBO Rep. **4:**761–765.
34. **Kalff-Suske, M., et al.** 1999. Point mutations throughout the GLI3 gene cause Greig cephalopolysyndactyly syndrome. Hum. Mol. Genet. **8:**1769–1777.
35. **Kang, S., J. M. Graham, Jr, A. H. Olney, and L. G. Biesecker.** 1997. GLI3 frameshift mutations cause autosomal dominant Pallister-Hall syndrome. Nat. Genet. **15:**266–268.
36. **Kinzler, K. W., et al.** 1987. Identification of an amplified, highly expressed gene in a human glioma. Science **236:**70–73.
37. **Kinzler, K. W., J. M. Ruppert, S. H. Bigner, and B. Vogelstein.** 1988. The GLI gene is a member of the Kruppel family of zinc finger proteins. Nature **332:**371–374.
38. **Knepper, J. L., A. C. James, and J. E. Ming.** 2006. TGIF, a gene associated with human brain defects, regulates neuronal development. Dev. Dyn. **235:** 1482–1490.
39. **Kuang, C., et al.** 2006. Intragenic deletion of Tgif causes defects in brain development. Hum. Mol. Genet. **15:**3508–3519.
40. **Lee, J., K. A. Platt, P. Censullo, and A. Ruiz i Altaba.** 1997. Gli1 is a target of Sonic hedgehog that induces ventral neural tube development. Development **124:**2537–2552.
41. **Lei, Q., A. K. Zelman, E. Kuang, S. Li, and M. P. Matise.** 2004. Transduction of graded Hedgehog signaling by a combination of Gli2 and Gli3 activator functions in the developing spinal cord. Development **131:**3593–3604.
42. **Litingtung, Y., and C. Chiang.** 2000. Specification of ventral neuron types is mediated by an antagonistic interaction between Shh and Gli3. Nat. Neurosci. **3:**979–985.
43. **Liu, F., J. Massague, and A. Ruiz i Altaba.** 1998. Carboxy-terminally truncated Gli3 proteins associate with Smads. Nat. Genet. **20:**325–326.
44. **Margulies, E. H., M. Blanchette, D. Haussler, and E. D. Green.** 2003. Identification and characterization of multi-species conserved sequences. Genome Res. **13:**2507–2518.
45. **Marigo, V., R. L. Johnson, A. Vortkamp, and C. J. Tabin.** 1996. Sonic hedgehog differentially regulates expression of GLI and GLI3 during limb development. Dev. Biol. **180:**273–283.
46. **Marine, J.-C., E. J. Bellefoid, H. Pendeville, J. A. Martial, and T. Pieler.** 1997. A role for Xenopus Gli-type zinc-finger proteins in the early embbryonic patterning of the mesoderm and neuroectoderm. Mech. Dev. **63:**211–225.
47. **McDermott, A., et al.** 2005. Gli2 and Gli3 have redundant and context-dependent function in skeletal muscle formation. Development **132:**345–357.
48. **McMahon, A. P., P. W. Ingham, and C. J. Tabin.** 2003. Developmental roles and clinical significance of hedgehog signaling. Curr. Top. Dev. Biol. **53:**1–114.
49. **Meyer, N. P., and H. Roelink.** 2003. The amino-terminal region of Gli3 antagonizes the Shh response and acts in dorsoventral fate specification in the developing spinal cord. Dev. Biol. **257:**343–355.
50. **Mo, R., et al.** 1997. Specific and redundant functions of Gli2 and Gli3 zinc finger genes in skeletal patterning and development. Development **124:**113–123.
51. **Mukherjee, K., and T. R. Burglin.** 2007. Comprehensive analysis of animal TALE homeobox genes: new conserved motifs and cases of accelerated evolution. J. Mol. Evol. **65:**137–153.
52. **Mullor, J. L., N. Dahmane, T. Sun, and A. Ruiz i Altaba.** 2001. Wnt signals are targets and mediators of Gli function. Curr. Biol. **11:**769–773.
53. **Neuteboom, S. T., and C. Murre.** 1997. Pbx raises the DNA binding specificity but not the selectivity of antennapedia Hox proteins. Mol. Cell. Biol. **17:**4696–4706.
54. **Paparidis, Z., et al.** 2007. Ultraconserved non-coding sequence element controls a subset of spatiotemporal GLI3 expression. Dev. Growth Differ. **49:**543–553.
55. **Park, H. L., et al.** 2000. Mouse Gli1 mutants are viable but have defects in SHH signaling in combination with a Gli2 mutation. Development **127:**1593–1605.
56. **Persson, M., et al.** 2002. Dorsal-ventral patterning of the spinal cord requires Gli3 transcriptional repressor activity. Genes Dev. **16:**2865–2878.
57. **Radhakrishna, U., et al.** 1999. The phenotypic spectrum of GLI3 morphopathies includes autosomal dominant preaxial polydactyly type-IV and postaxial polydactyly type-A/B; no phenotype prediction from the position of GLI3 mutations. Am. J. Hum. Genet. **65:**645–655.
58. **Radhakrishna, U., A. Wild, K. H. Grzeschik, and S. E. Antonarakis.** 1997. Mutation in GLI3 in postaxial polydactyly type A. Nat. Genet. **17:**269–271.
59. **Ruppert, J. M., et al.** 1988. The GLI-Kruppel family of human genes. Mol. Cell. Biol. **8:**3104–3113.
60. **Saleh, M., I. Rambaldi, X. J. Yang, and M. S. Featherstone.** 2000. Cell signaling switches HOX-PBX complexes from repressors to activators of transcription mediated by histone deacetylases and histone acetyltransferases. Mol. Cell. Biol. **20:**8623–8633.
61. **Sasaki, H., Y. Nishizaki, C.-C. Hui, M. Nakafuku, and H. Kondoh.** 1999. Regulation of Gli2 and Gli3 activities by an amino-terminal repression domain: implication of Gli2 and Gli3 as primary mediators of Shh signaling. Development **126:**3915–3924.
62. **Selleri, L., et al.** 2001. Requirement for Pbx1 in skeletal patterning and programming chondrocyte proliferation and differentiation. Development **128:**3543–3557.
63. **Swartz, M., J. Eberhart, G. S. Mastick, and C. E. Krull.** 2001. Sparking new frontiers: using in vivo electroporation for genetic manipulations. Dev. Biol. **233:**13–21.
64. **Tagle, D. A., et al.** 1988. Embryonic epsilon and gamma globin genes of a prosimian primate (Galago crassicaudatus). Nucleotide and amino acid sequences, developmental regulation and phylogenetic footprints. J. Mol. Biol. **203:**439–455.
65. **te Welscher, P., M. Fernandez-Teran, M. A. Ros, and R. Zeller.** 2002. Mutual genetic antagonism involving GLI3 and dHAND prepatterns the vertebrate limb bud mesenchyme prior to SHH signaling. Genes Dev. **16:**421–426.
66. **Tyurina, O. V., et al.** 2005. Zebrafish Gli3 functions as both an activator and a repressor in Hedgehog signaling. Dev. Biol. **277:**537–556.
67. **Ulloa, F., N. Itasaki, and J. Briscoe.** 2007. Inhibitory Gli3 activity negatively regulates Wnt/beta-catenin signaling. Curr. Biol. **17:**545–550.
68. **Vokes, S. A., H. Ji, W. H. Wong, and A. P. McMahon.** 2008. A genome-scale analysis of the cis-regulatory circuitry underlying sonic hedgehog-mediated patterning of the mammalian limb. Genes Dev. **22:**2651–2663.
69. **von Mering, C., and K. Basler.** 1999. Distinct and regulated activities of human Gli proteins in Drosophila. Curr. Biol. **9:**1319–1322.
70. **Vortkamp, A., M. Gessler, and K. H. Grzeschik.** 1991. GLI3 zinc-finger gene interrupted by translocations in Greig syndrome families. Nature **352:**539–540.
71. **Wang, B., J. F. Fallon, and P. A. Beachy.** 2000. Hedgehog-regulated processing of Gli3 produces an anterior/posterior repressor gradient in the developing vertebrate limb. Cell **100:**423–434.
72. **Wild, A., et al.** 1997. Point mutations in human GLI3 cause Greig syndrome. Hum. Mol. Genet. **6:**1979–1984.
73. **Wotton, D., R. S. Lo, L. A. Swaby, and J. Massague.** 1999. Multiple modes of repression by the Smad transcriptional corepressor TGIF. J. Biol. Chem. **274:**37105–37110.
74. **Yee, S. P., and P. W. Rigby.** 1993. The regulation of myogenin gene expression during the embryonic development of the mouse. Genes Dev. **7:**1277–1289.
75. **Zhang, X., A. Friedman, S. Heaney, P. Purcell, and R. L. Maas.** 2002. Meis homeoproteins directly regulate Pax6 during vertebrate lens morphogenesis. Genes Dev. **16:**2097–2107.